

Collective Phenomena in Heavy Ion Collisions

M. Petrovici* and A. Pop

*National Institute of Physics and Nuclear Engineering
P.O.Box MG-6, Bucharest-Magurele, Romania*

(Dated: October 29, 2018)

A review of the main results of detailed flow analysis in highly central and semi-central heavy ion collisions at SIS energies is presented in the first part of this paper. The influence of the mass of the colliding nuclei and centrality on the collective expansion and the information on the equation of state of compressed and hot baryonic matter is discussed. The second part is dedicated to a similar type of analysis, based on the behaviour of the average transverse momentum as a function of mass of different hadrons, at the other extreme of energy range, where free baryonic fireballs are produced. Information on the partonic and hadronic expansion, temperature and degree of thermal equilibrium in p+p and Au+Au central collisions at 200 A·GeV is presented.

PACS numbers: 25.75.-q,25.75.Ld,25.70.Pq,05.20.-y,05.90+m

I. INTRODUCTION

As far as the new states of matter are obtained in laboratory using heavy ion collisions, it is mandatory to have as much as possible under control the finite size and dynamical aspects. One of these is the dynamical evolution of the transient piece of matter produced in heavy ion collisions. The present experimental evidence supports the existence of collective expansion caused by the pressure gradients built-up during the first phase of the collision. Understanding this expansion one could aim to pin down the properties of the initial phase of matter, before expansion and at the same time, to extract information on in-medium effects, equation of state or phase transitions.

Results of a detailed analysis of the expansion properties of hot and compressed baryonic matter at SIS energies in highly central and mid-central heavy ion collisions will be presented in Chapters I and II, respectively. Chapter III presents results of a similar analysis in terms of collective expansion and temperature at RHIC energies, in the free baryonic sector. Preliminary results seem to support the possibility to disentangle between the contributions coming from partonic and hadronic phases and to access information on the degree of thermal equilibration of these two stages of expanding matter formed in central collisions at 200 A·GeV. Conclusions will be presented in Chapter IV.

II. HIGHLY CENTRAL SYMMETRIC COLLISIONS

For the highly central Au + Au collision at 150 A·MeV incident energy [1], the mean kinetic energy of fragments divided by their mass, was observed to present a dependence as a function of atomic charge which deviates from the one typical for a thermal plus Coulomb scenario. This

experimental trend agrees rather well with a thermal motion superimposed onto a collective velocity field which in the non-relativistic limit can be written as:

$$\langle E_{kin}^{cm} \rangle = \frac{1}{2} A \cdot m_0 \cdot \langle \beta_{flow}^2 \rangle + \frac{3}{2} T'' \quad (1)$$

$\frac{1}{2} m_0 \cdot \langle \beta_{flow}^2 \rangle$ is the flow energy per nucleon and T'' stands for the effect of non-explicit treatment of Coulomb effects in the above expression. This leads systematically to an overestimated value of the real temperature T [2]. While this trend was qualitatively reproduced by the QMD microscopic transport model [3], the absolute value of mean kinetic energy per nucleon is systematically underestimated for all fragments. The experimental values were reproduced rather well by a hybrid model based on hydrodynamical expansion coupled with a statistical fragmentation at the break-up moment [4]. This supports the model prediction that different species originate with different probabilities as a function of position within the fireball and time, heavier fragments being emitted later, at lower temperature and lower expansion. This was confirmed in the meantime by small angle correlations studies for pairs of nonidentical reaction species [5],[6]. A detailed analysis of experimental FOPI-Phase II data based on the equation above was performed for three symmetric systems (Au+Au, Xe + CsI, Ni + Ni), different incident energies and two regions of polar angles in the center of mass system for highly central collisions [7],[8]. While in the forward polar region, $25^\circ \leq \theta_{cm} \leq 45^\circ$, all three systems show the same flow at all measured energies, along the transverse direction and mid-rapidity, i.e. $80^\circ \leq \theta_{cm} \leq 100^\circ$, the collective expansion is lower, its dependence on the incident energy is not that steep and at the same incident energy the collective expansion increases with the mass of the colliding system. Calculations based on IQMD model at 250 A·MeV showed that the nucleons emitted at 90° suffer in the average 3.5 collisions relative to 1.7 of those emitted at smaller polar angles. This tells that at 90° the observed effect is most probably coming from an equilibrated fireball, while at forward angles the Corona effects and uncertainty in im-

*Electronic address: mpetro@nipne.ro

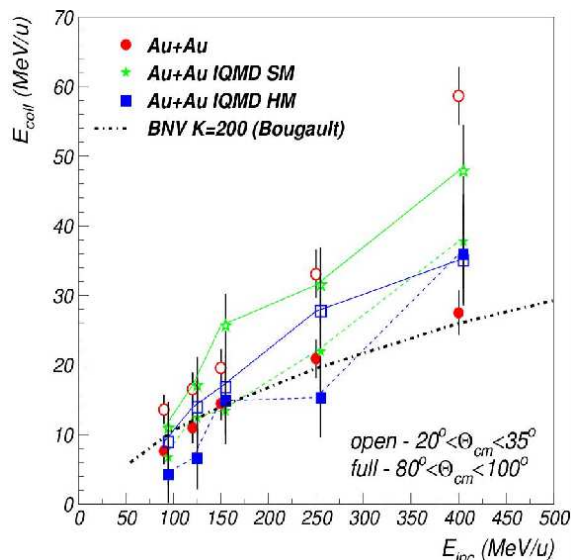


FIG. 1: Collective energy, E_{coll} , as a function of incident energies in highly central Au+Au collisions (1% total cross section). Open circles $25^\circ \leq \theta_{cm} \leq 45^\circ$, full circles $80^\circ \leq \theta_{cm} \leq 100^\circ$. IQMD predictions are represented by open and full squares for hard equation of state (HM) and open and full stars for soft equation of state (SM), for the corresponding polar regions. BNV prediction using a soft equation of state is represented by dotted dashed line

parameter selection play an important role. Experimental slopes obtained for highly central Au+Au collisions, 1% total cross section, selected using the ratio of transverse and longitudinal energies of all detected and identified charged particles ($E_{rat} = \sum_i E_{\perp,i} / \sum_i E_{\parallel,i}$ in the c.m. system) presented in Fig. 1 [9], support the microscopic transport model estimates, IQMD [3] and BNV [10] based on soft equation of state.

III. MID-CENTRAL COLLISIONS

What else could one learn at these incident energies going to mid-central collisions? As far as concerns the centrality dependence of collective expansion one has to be aware that an average on azimuth (Fig. 2) automatically includes contribution coming from shadowing effects due to spectator matter while the values extracted at 90° (Fig. 3) are strongly influenced by the aspect ratio of the fireball. With this in mind, one can see a systematic increase of flow energy with the centrality (A_{part} estimated in a sharp cut-off geometrical model) the effect being more pronounced at the higher measured incident energies. A detailed analysis of the collective expansion azimuthal distributions at mid-rapidity, different impact parameters and incident energies for Au + Au and Xe + CsI has been done by the FOPI Collaboration [11]. The qualitative agreement between the predictions of the model based on hydrodynamical expansion coupled with a statistical fragment formation at the break-up moment

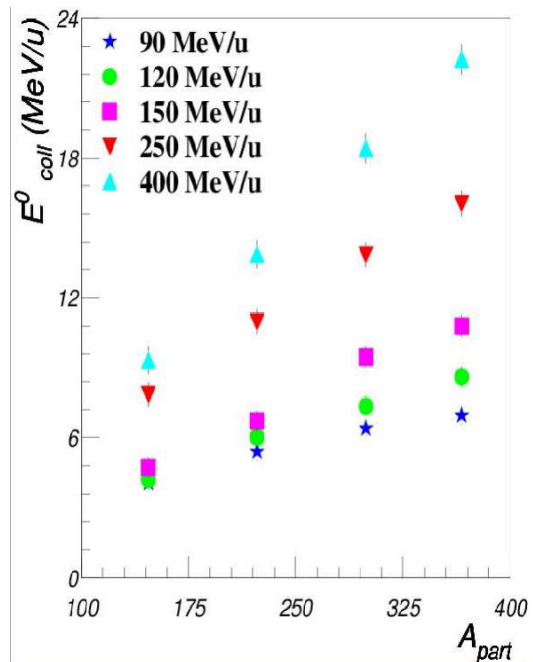


FIG. 2: Azimuthally averaged E_{coll} as a function of A_{part} for Au+Au collisions at 90, 120, 150, 250 and 400 A·MeV and $80^\circ \leq \theta_{cm} \leq 100^\circ$.

[4], under the hypothesis that the expansion starts at the maximum overlap and perfect shadowing of the spectator matter, let us to conclude that different regions of azimuth capture different periods of central fireball expansion [6],[11]. If this is the case, then the amplitude of the azimuthal oscillation of E_{coll} is recommended as a sensitive observable to the equation of state of hot and compressed baryonic matter produced at these energies. Transport model calculations based on BUU code [12] using momentum dependent mean fields ($m^*/m=0.79$), in-medium elastic cross sections ($\sigma = \sigma_0 \tanh(\sigma^{free}/\sigma_0)$ with $\sigma_0 = \rho^{-2/3}$) and soft (K=210 MeV, gray zone) or stiff (K=380 MeV, dashed zone) EoS are compared in Fig. 4 and Fig. 5 with the experimental results. One should mention that the light fragments (up to A=3) are produced in a few-nucleon processes inverse to composite break-up, relative to the general coalescence recipe used by microscopic transport codes.

The measured relative yields are nicely reproduced by this model, especially at higher incident energies [2]. For comparison with the experiment, the calculated azimuthal distribution has been smeared according to the measured reaction-plane dispersion values. The azimuthal distribution of the average kinetic energy of different species and of the collective energy per nucleon extracted from these were fitted with:

$$\langle E_{kin} \rangle = E_{kin}^0 - \Delta E_{kin} \cdot \cos 2\Phi \quad (2)$$

and

$$E_{coll} = E_{coll}^0 - \Delta E_{coll} \cdot \cos 2\Phi \quad (3)$$

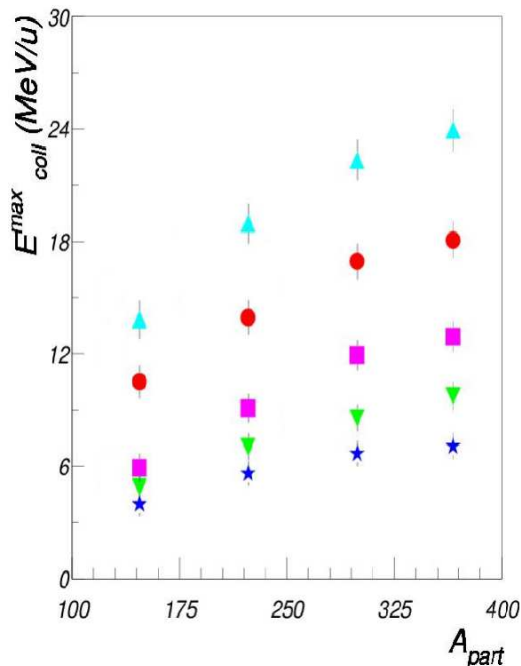


FIG. 3: E_{coll} as a function of A_{part} for Au+Au collisions at 90, 120, 150, 250 and 400 A·MeV, $80^\circ \leq \theta_{cm} \leq 100^\circ$ and $72^\circ \leq \phi \leq 108^\circ, 252^\circ \leq \phi \leq 288^\circ$ (same symbols as in Fig. 2)

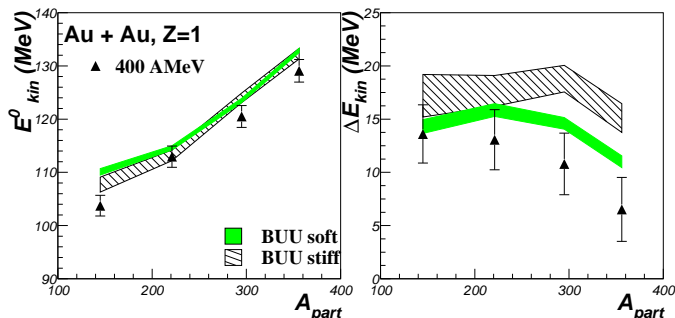


FIG. 4: E_{kin}^0 and ΔE_{kin} as a function of A_{part} , for $Z=1$ ($A=1,2,3$) fragments, Au+Au at 400 A·MeV. The experimental results are represented by triangles, while the BUU results are represented by gray zones for soft EoS and by dashed zones for stiff EoS, respectively.

respectively. As one could see in these figures, E_{kin}^0 for $Z=1$ ($A=1,2,3$) fragments (Fig. 4) and E_{coll}^0 (Fig. 5) are very little sensitive to the equation of state, both EoS parameterizations showing quite good agreement with the data. As far as concerns ΔE_{kin} and ΔE_{coll} , the calculations with the soft EoS reproduce the overall trends of the experiment while the calculations with the stiff EoS overestimate significantly the ΔE_{kin} and ΔE_{coll} values at higher and lower centralities, respectively. The results presented above support the conclusion that the equation of state of baryonic matter at densities of about $2\rho_0$ and temperatures of about 50-70 MeV is soft. This conclusion seems to be also supported by kaon production in heavy

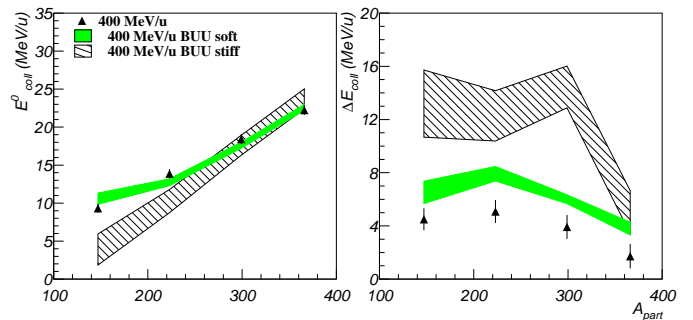


FIG. 5: E_{coll}^0 and ΔE_{coll} as a function of A_{part} , for Au+Au at 400 A·MeV. The symbols have the same interpretation as in Fig. 4.

ion collisions as it was shown by KAOS Collaboration [13].

IV. TOWARDS BARYONIC FREE MATTER

The experimental information obtained at AGS, SPS and RHIC energies confirmed that the particle distributions reflect mainly the conditions reached by the system in its final state. Therefore, information originating from earlier stages is mandatory in order to conclude whether the system passed through a partonic phase and extract information on such a phase. In central collisions, the final collective transverse, azimuthally isotropic flow, cumulates any collective flow generated during the evolution of the fireball, i.e. from the partonic and hadronic phases, the yield ratios reflecting mainly the statistical nature of the hadronization process. This was nicely shown at RHIC, by the STAR Collaboration [14], by analyzing the transverse momentum distribution for common and rare particles using the blast wave model. The extracted kinetic freeze-out temperature and the flow velocity show a clear dependence as a function of centrality while the chemical freeze-out temperature, extracted from particle yield ratios using statistical model stays constant, at about 170 MeV. At the same time the data seem to indicate a sequential freeze-out of particles, hyperons decoupling from the system earlier at temperatures closer to the chemical temperature value. As we have seen in the first part of the present paper, a useful observable for a detailed study of collective flow would be the mean kinetic energy as a function of mass of different species. In the following we shall present the results of a similar analysis, this time in terms of the average transverse momentum $\langle p_t \rangle$ as a function of hadron mass for different colliding systems and energies. A careful examination of the experimental $\langle p_t \rangle$ values [15] as a function of mass for π^\pm , K^\pm , p and \bar{p} evidences that the slope increases going from p+p to Cu+Cu and Au+Au at the same incident energy, i.e. 200 A·GeV. Although less pronounced, similar trend is observed as a function of inci-

dent energy for a given system [16]. In order to extract quantitative information we used the blast wave model for calculating the $\langle p_t \rangle$ as a function of mass:

$$\langle p_t \rangle = \frac{\int_0^\infty p_t^2 f(p_t) dp_t}{\int_0^\infty p_t f(p_t) dp_t} \quad (4)$$

where:

$$f(p_t) \sim \int_0^R r dr m_t I_0 \left(\frac{p_t \sinh \rho}{T} \right) K_1 \left(\frac{m_t \cosh \rho}{T} \right) \quad (5)$$

$$\rho = \tanh^{-1} \beta_r \quad (6)$$

and

$$\beta_r(r) = \beta_s \left(\frac{r}{R} \right) \quad (7)$$

The temperature T and expansion velocity β_s were the free parameters used to fit the experimental $\langle p_t \rangle$ as a function of mass [17]. Within this ansatz $\beta = \frac{2}{3}\beta_s$. The results are presented in Fig. 6. The left part shows the

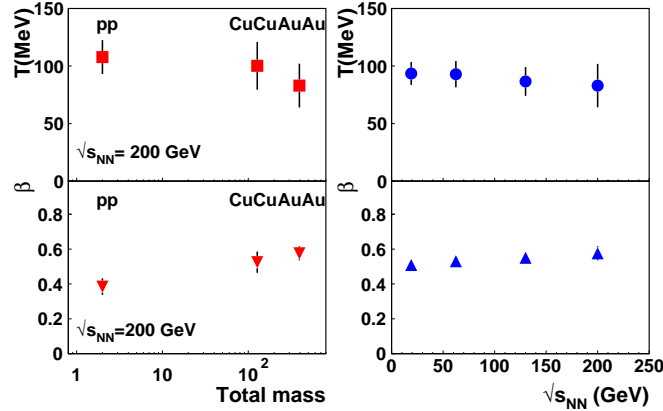


FIG. 6: Left part: the temperature T and expansion velocity β as a function of total mass of the colliding system at 200 A·GeV; Right part: the temperature and β for Au + Au as a function of center of mass energy per nucleon.

temperature and expansion velocity β as a function of total mass of the colliding system at 200 A·GeV and the right part the temperature and β for Au + Au as a function of center of mass energy per nucleon. The temperature drops by ~ 20 MeV and the expansion velocity is increasing from p+p towards heavy systems. Although the decrease in temperature is moderate it is consistent with the interpretation that stronger expansion observed in heavier combinations cools down the fireball and therefore the final, kinetic break-up temperature is lower. Let's look now to $\langle p_t \rangle$ as a function of

mass for all particles measured by the STAR Collaboration at 200 A·GeV for p+p and Au+Au collisions [18] presented in Fig. 7. The two lines represent the results of the fits using the above expressions for p+p (dark line)

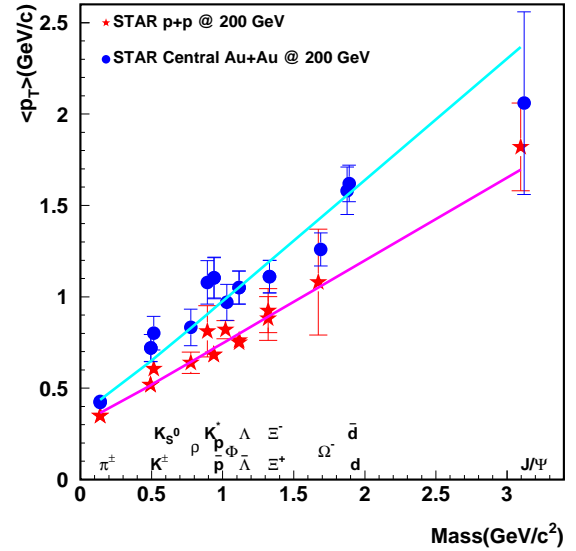


FIG. 7: Mid-rapidity average transverse momentum as a function of mass of different particles measured by STAR Collaboration.

and Au+Au (gray line). The corresponding temperatures and β values are: $T=111.6 \pm 23.8$ MeV and $\beta=0.39 \pm 0.06$ for p+p and $T=109.8 \pm 16.5$ MeV and $\beta=0.50 \pm 0.04$ for Au+Au. While the freeze-out kinetic temperature seems to be similar for p+p and Au+Au, the expansion is much more violent in the Au+Au case. If for Au+Au one considers only π^\pm , K^\pm , K^* , K_s^0 , p , \bar{p} , d , \bar{d} particles, the obtained temperature is $T=98.7 \pm 19.5$ MeV and $\beta=0.54 \pm 0.04$. It is well known that for understanding the particle production in high energy and nuclear physics, many authors used Tsallis statistics [19]. Tsallis' generalization of Boltzmann-Gibbs extensive statistics, based on the definition of a q-deformed entropy functional, is supposed to be adequate for describing systems characterized by memory effects and long range-interactions. The Boltzmann-Gibbs statistics is recovered in the limit $q \rightarrow 1$, therefore $(q-1)$ is interpreted as a measure of the degree of non-equilibrium, the temperature T being interpreted as the average temperature. If we replace in Eq. (4), $f(p_t)$ with the distribution corresponding to the blast wave model in which the Tsallis statistics has been implemented [20], [21]:

$$f(p_t) = m_T \int_{-Y}^Y \cosh(y) dy \int_{-\pi}^{\pi} d\phi \int_0^R r dr \left(1 + \frac{q-1}{T} (m_T \cosh(y) \cosh(\rho) - p_t \sinh(\rho) \cos(\phi))\right)^{-1/(q-1)} \quad (8)$$

and fit the same experimental data with the new expression, the results presented in Fig. 8 are obtained. For

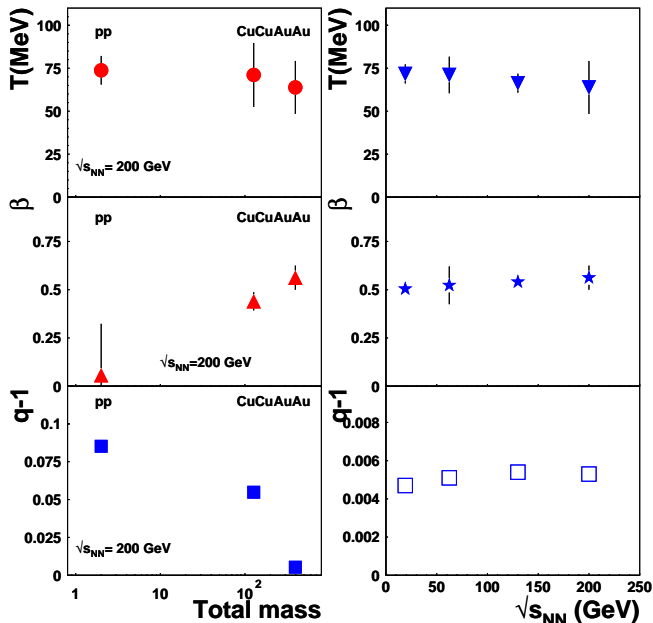


FIG. 8: Left part: the temperature T , expansion velocity β and q parameters as a function of total mass of the colliding system at 200 A·GeV; Right part: the temperature, β and $(q-1)$ parameters for Au + Au as a function of center of mass energy per nucleon.

TABLE I:

System	p + p	p + p	Au + Au	Au + Au
Model	BGBW	TBW	BGBW	TBW
T	111.6 ± 23.8	78.86 ± 10.13	109.8 ± 16.5	86.8 ± 1.54
β	0.39 ± 0.06	0.027 ± 0.10	0.50 ± 0.04	0.48 ± 0.04
q	1.0	1.087 ± 0.002	1.0	1.025 ± 0.003

p+p the boosted Tsallis scenario gives a negligible expansion velocity. As far as concerns the q parameter, one could observe a strong decrease as a function of total mass of the colliding system, large deviation from Boltzmann statistics, $(q-1) \simeq 0.085$, for p+p to relative small value, 0.005, for Au+Au being observed. The value for Au+Au stays almost constant, $\simeq 0.005$ as a function of incident energy. One should mention that a similar trend as a function of incident energy but for larger $(q-1)$ values was observed in e^+e^- collision, obtained from analyzing the p_t spectra in terms of simple, not boosted, Tsallis distribution [22].

If all species are considered, as in Fig. 7, the results of the fit are summarized in Table I where the blast wave models with Boltzmann-Gibbs (BGBW) and respectively Tsallis (TBW) statistics are compared. β is almost zero, therefore no expansion is built up in p+p collision at 200 A·GeV and the degree of non-equilibrium is about a factor of four larger in p+p relative to Au+Au. For Au+Au the extracted temperature is about 20 MeV lower and β is within the error bars similar with the one obtained using the blast wave model with Boltzmann statistics scenario. If one considers separately common particles, i.e. hadrons with larger interaction cross section, the results are presented in Table II. The temperature de-

TABLE II:

	Au + Au	Au + Au
	BGBW	TBW
T [MeV]	98.7 ± 19.5	79.05 ± 0.04
β	0.54 ± 0.04	0.53 ± 0.0005
q	1.0	1.0175 ± 0.0018

creases, β slightly increases and the deviation from Boltzmann statistics is reduced. If we consider only the hyperons and J/Ψ , as it is shown in Table III, a temperature around 200 MeV, $\beta \simeq 0.3$ and larger deviation from global equilibrium is obtained. This suggests that strange

TABLE III:

	Au + Au
	TBW
T [MeV]	198.0 ± 7.6
β	0.32 ± 0.012
q	1.0247 ± 0.0043

and heavy flavour hadrons keep the characteristics of expansion at the hadronization moment, characterized by lower values of β , higher temperature and based on Tsallis statistics interpretation, not fully equilibrated. After hadronization, strongly interacting particles, within still highly dense environment continue to build up expansion, cooling down the system and approaching a global equilibrium.

The Minuit package was used to perform the least χ^2 fit. The quality of the fit was reasonably good as can be seen in Fig. 9, where $1/\chi^2$ is represented as a function of two pairs of parameters for the result of the fit listed in Table III.

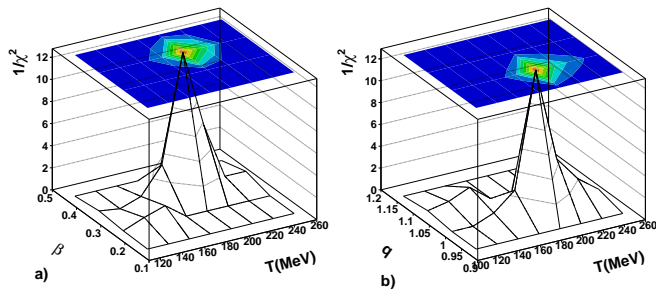


FIG. 9: a) $1/\chi^2$ as a function of temperature and β ; b) $1/\chi^2$ as a function of temperature and q for the result of the fit listed in Table III.

V. CONCLUSIONS

In this paper we tried to present a short review of the main results of detailed flow analysis at incident energies where compressed and hot baryonic fireballs are produced. The experimental data support model predictions that different species originate with different probabilities as a function of position within the fireball and time, heavier fragments being emitted later, at lower temperature and lower expansion. The best agreement between experiment and theoretical estimates based on microscopic transport models is obtained if a soft equation of state is considered.

Similar type of analysis extended at the other extreme of incident energies, where free baryonic matter is

produced, shows that for central collisions, azimuthally isotropic flow of different species could be used to pin down the relative contributions coming from partonic and hadronic levels. The kinetic temperature and expansion velocity extracted from experimental $\langle p_t \rangle$ dependence on the hadron mass using boosted Boltzmann and Tsallis expressions support the conclusion that strange and heavy flavour hadrons carry the information from the partonic stage characterized by higher temperature and lower expansion. The results based on boosted Tsallis distribution (within the limits of its applicability and interpretation) indicate high degree of non-equilibrium and missing expansion in pp collisions at RHIC energy. For the Au+Au collision similar analysis for strange and heavy flavour hadrons gives a higher temperature, less violent expansion and higher degree of non-equilibrium of the initial, deconfined matter produced at the highest RHIC energy. Common hadrons, strongly interacting after hadronization, continue to build up expansion, cool down the system and bring it towards a global equilibrium.

It is a real challenge for the near future experiments at LHC to use the potentiality of flow phenomena to extract new physics in an energy domain of about 30 times larger than the one attainable at RHIC. Preliminary results based on Monte Carlo simulations show that the ALICE experiment is able to reconstruct with high accuracy the p_t distribution for most of the particles making the type of analysis presented in this paper feasible and promising.

-
- [1] S. C. Jeong and FOPI Collaboration, Phys. Rev. Lett. 72 (1994) 3468
- [2] G. Poggi and FOPI Collaboration, Nucl. Phys. A 586 (1995) 755
- [3] C. Hartnack et al., Phys. Lett. B 336 (1994) 131; Mod.Phys.Lett. A9 (1994) 1151
- [4] M. Petrovici and FOPI Collaboration, Phys. Rev. Lett. 74 (1995) 5001
- [5] R. Kotte and FOPI Collaboration, Eur. Phys. J. A 6 (1999) 185
- [6] M. Petrovici, Fizika B 12 (2003) 165
- [7] M. Petrovici and FOPI Collaboration, Clustering Aspects of Nuclear Structure and Dynamics, ISBN 981-02-4233-6, World Scientific 2000, p.337
- [8] M. Petrovici and FOPI Collaboration, Advances in Nuclear Physics, ISBN 981-02-4276-X, World Scientific 2000, p.242
- [9] G. Stoicea, PhD Thesis - Bucharest 2003
- [10] R. Bougault et al., Nouvelles de GANIL, no.58, 1996
- [11] G. Stoicea and FOPI Collaboration, Phys. Rev. Lett. 92 (2004) 072303
- [12] P. Danielewicz and Q. Pan, Phys. Rev. C 46 (1992) 2002, P. Danielewicz, Nucl. Phys. A 673 (2000) 375
- [13] C. Sturm and KAOS Collaboration, Phys. Rev. Lett. 86 (2001) 39
- [14] O. Barannikova and STAR Collaboration, nucl-ex/0403014
- [15] B. I. Abelev and STAR Collaboration, Phys. Rev. C 79 (2009) 034909
- [16] M. Petrovici and A. Pop, AIP Conference Proceedings 972, p.98, 2008
- [17] E. Schnedermann, J. Solfrank and W.Heinz, Phys. Rev. C 48 (1993) 2462
- [18] B. I. Abelev and STAR Collaboration, Phys. Rev. C 75 (2007) 06490
- [19] C. Tsallis, J. Stat. Physics 52 (1988) 479
- [20] A. Lavagno, Phys. Lett. A 301 (2002) 13
- [21] Z. Tang, nucl-ex/0812.1609
- [22] I. Bediaga et al, Physica A 286 (2000) 156